Numerical Investigation of Thermal-Hydraulic Phenomena for SBLOCA in SMART-ITL

S. J. An [a*], Y. J. Lee [a], Y. J. Chung [a], S. W. Lim [a], H. Bae [a]
[a]*Korea Atomic Energy Research Institute, 1045 Daedeok-daero, Yuseong-gu, Daejeon, 305-353, Republic of Korea*
[*]*Corresponding author: sjan177@kaeri.re.kr*

1. Introduction

Recently, small modular reactor (SMR) has been attracting attention in various aspects such as safety, usability, and convenience of construction. For this reason, various SMRs have been developed in many foreign countries such as USA, Russia and China.

System-integrated modular advanced reactor (SMART) which is a SMR was developed by the Korea Atomic Energy Research Institute (KAERI) for the electricity generation and seawater desalination. SMART adopts a fully passive safety system consisted of four trains of passive safety injection system (PSIS), four trains of passive residual heat removal system (PRHRS) and Containment Pressure and Radioactivity Suppression System (CPRSS).

An integral-effect test loop for SMART (SMART-ITL) [1] was designed for various tests to understand the integral thermal-hydraulic behavior expected to occur in SMART. The SMART-ITL is equipped with PSIS and PRHRS except for CPRSS. The obtained experimental data is also used to validate the performance of the thermal-hydraulic code for the safety analysis.

In the present study, an attempt was made to numerically predict the thermal-hydraulic phenomena in SMART-ITL. For this purpose, TASS/SMR-S code [2] which is a one-dimensional thermal-hydraulic code for the safety and performance analysis was used. The simulation was performed for the small break loss of coolant accident (SBLOCA) on the safety injection (SI) line. The predicted results were compared with the experimental data.

2. Governing equations

The governing equations of the TASS/SMR-S code are consisted of mass conservation equations for mixture, liquid and non-condensable gas, a momentum conservation equation for mixture and energy conservation equations for mixture and gas as follows:

$$\begin{aligned}
&AL\frac{\partial \rho_m}{\partial t^*}+AL\frac{\partial \rho_m}{\partial t}+L\frac{\partial}{\partial x}\left[(1-\alpha)\rho_l u_l A+\alpha\rho_g u_g A\right]=0\\
&AL\frac{\partial}{\partial t^*}\left[(1-\alpha)\rho_l\right]+AL\frac{\partial}{\partial t}\left[(1-\alpha)\rho_l\right]+L\frac{\partial}{\partial x}\left[(1-\alpha)\rho_l u_l A\right]=\Gamma\\
&AL\frac{\partial}{\partial t^*}(\alpha\rho_n)+AL\frac{\partial}{\partial t}(\alpha\rho_n)+L\frac{\partial}{\partial x}(\alpha\rho_n u_g A)=0
\end{aligned}\tag{1}$$

$$\begin{aligned}
&AL\frac{\partial}{\partial t^*}(\rho_m u_m)+AL\frac{\partial}{\partial t}(\rho_m u_m)+L\frac{\partial}{\partial x}\left[(1-\alpha)\rho_l u_l u_l A+\alpha\rho_g u_g u_g A\right]=\\
&\qquad -AL\frac{\partial P}{\partial x}-F_{fric}-F_{form}-F_{grav}
\end{aligned}\tag{2}$$

$$\begin{aligned}
&AL\frac{\partial}{\partial t^*}(\rho_m e_m)+AL\frac{\partial}{\partial t}(\rho_m e_m)+L\frac{\partial}{\partial x}\left[(1-\alpha)\rho_l h_l u_l A+\alpha\rho_g h_g u_g A\right]=\dot{Q}_w\\
&AL\frac{\partial}{\partial t^*}(\alpha\rho_g e_g)+AL\frac{\partial}{\partial t}(\alpha\rho_g e_g)+L\frac{\partial}{\partial x}(\alpha\rho_g h_g u_g A)+ALP\frac{\partial\alpha}{\partial t}=\dot{Q}_g-\Gamma h_s
\end{aligned}\tag{3}$$

where t is the physical time for transient calculations, and t^* is the pseudo time for internal iterations to get the converged solutions at every physical time stage.

The drift-flux model [3] was used to estimate the velocity of each phase. The Henry-Fauske model [4] was adopted to determine the critical flow rate at the break.

3. Numerical methods

The Governing equations were applied to the given nodalizations, shown in Fig. 1, using a staggered grid concept, and was discretized based on a semi-implicit method. The inviscid flux terms were discretized using an upwind method. The approximated Jacobian was adopted for the implicit operator in momentum equation. For the transient time-accurate calculations, a dual-time stepping time integration algorithm based on a linearized first order Euler backward differencing was used by adopting a time-step size with pseudo-time sub-iterations.

4. Nodalization

In Fig. 1, the nodalization for the SMART-ITL with the PSIS is presented. The reactor coolant system (RCS), secondary system for the feedwater control valves to the turbine stop valves, safety injection tanks (SITs), core makeup tanks (CMTs), and the PRHRS are modeled. The entire computational domain is consisted of 406 nodes and 461 paths.

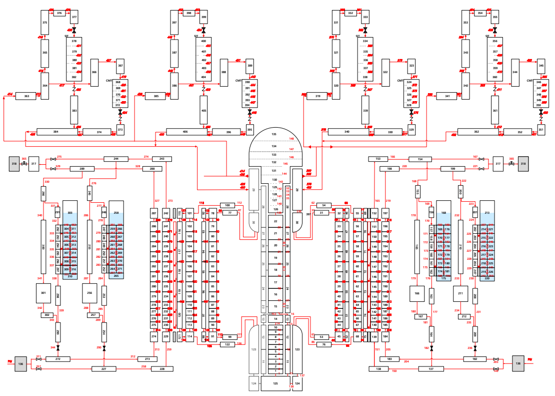

Fig. 1. Nodalization of SMART-ITL

5. Results

The prediction capability of the TASS/SMR-S code is evaluated using the test results of the SMART-ITL with regard to a SI line break. An assumption of critical flows is applied to the SIT isolation valve.

The break occurs at t = 0 sec, and the pressure decreases and reaches setpoint of reactor trip. The reactor coolant pumps begin to coastdown and the feedwater supply is stopped due to the loss of offsite power assumed simultaneously with the reactor trip. As the PRHR actuation signal is generated by the low feedwater flow rate, the PRHRS isolation valves are opened. After that, the safety injection water is supplied to recover the water level of the reactor pressure vessel. The transient behaviors of the major thermal-hydraulic parameters are described as follows.

In Fig. 2, the core power during the SI line break LOCA is presented. The test result showed that the core power decreased rapidly to the decay heat level due to reactor trip caused by the low pressurizer pressure (LPP). The reactor trip time by the LPP is predicted accurately.

In Fig. 3, the break flow rate is presented. The test results showed that the coolant was discharged rapidly through the break. The break flow rate formed a critical flow in the early phase of the accident and decreased as the system pressure decreased. The predicted break flow rate is reasonable.

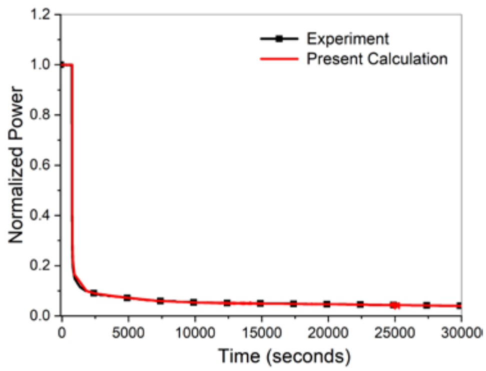

Fig. 2. Core power

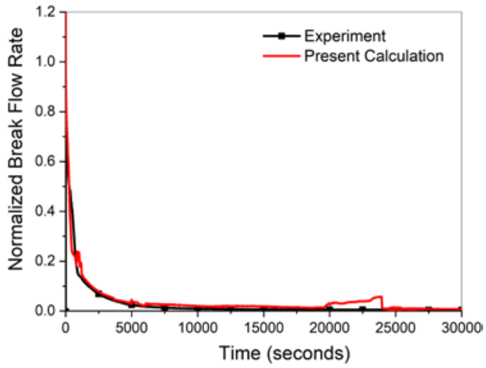

Fig. 3. Break flow rate

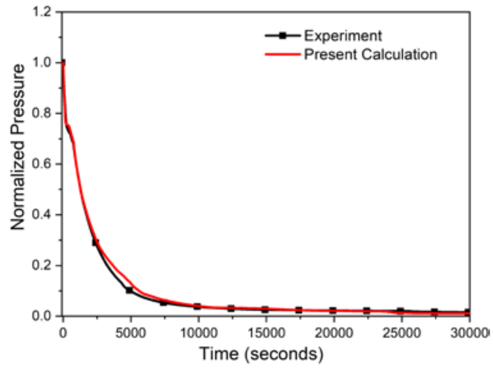

Fig. 4. Pressurizer pressure

In Fig. 4, the behavior of pressurizer (PZR) pressure is presented. When the SI line break occurred, the PZR pressure dropped quickly and the reactor trip signal by the LPP was generated. The system pressure decreased continuously after the reactor trip. The depressurization rate is predicted comparatively well.

6. Conclusions

In the present study, a numerical simulation was carried out to predict the thermal-hydraulic phenomena for SBLOCA in SMART-ITL. For this purpose, the TASS/SMR-S code was used. The calculation was made for the SI line break SBLOCA with the operation of PSIS. It was shown that the agreement between the prediction and test is reasonably good for the core power, break flow rate, and PZR pressure.

ACKNOWLEDGMENTS

This work was supported by the National Research Foundation of Korea (NRF) funded by the Ministry of Science and ICT. (2020M2D7A1079182)

REFERENCES

[1] H. Bae, D. E. Kim, S. U. Ryu, S. J. Yi, and H. S. Park, Comparison of three small-break loss-of-coolant accident tests with different break locations using the system-integrated modular advanced reactor-integral test loop facility to estimate the safety of the smart design, Nuclear Engineering and Technology, Vol. 49, No. 5, pp. 968-978, 2017.

[2] S. J. An, Y. J. Lee, and S. W. Lim, Development of a density-based algorithm for one-dimensional two-phase thermal hydraulic flows, 2021 KSCFE Spring Conference.

[3] B. Chexal, G. Lellouche, J. Horowitz, and J. Healzer, A void fraction correlation for generalized applications, Progress in Nuclear Energy, Vol. 27, No. 4, pp. 255-295, 1992.

[4] R. E. Henry, and H. K. Fauske, The two-phase critical flow of one-component mixtures in nozzles, orifice, and short tubes, Journal of Heat Transfer, Vol. 93, pp. 179-187, 1971.